

Alma Mater Studiorum Università di Bologna
Archivio istituzionale della ricerca

Comparison of Control Charts for Poisson Count Data in Healthcare Monitoring

This is the final peer-reviewed author's accepted manuscript (postprint) of the following publication:

Published Version:

Scagliarini, M., Boccaforno, N., Vandì, M. (2021). Comparison of Control Charts for Poisson Count Data in Healthcare Monitoring. APPLIED STOCHASTIC MODELS IN BUSINESS AND INDUSTRY, 37(1 (January/February)), 139-154 [10.1002/asmb.2560].

Availability:

This version is available at: <https://hdl.handle.net/11585/798318> since: 2021-02-11

Published:

DOI: <http://doi.org/10.1002/asmb.2560>

Terms of use:

Some rights reserved. The terms and conditions for the reuse of this version of the manuscript are specified in the publishing policy. For all terms of use and more information see the publisher's website.

This item was downloaded from IRIS Università di Bologna (<https://cris.unibo.it/>).
When citing, please refer to the published version.

(Article begins on next page)

Title

Comparison of Control Charts for Poisson Count Data in Healthcare Monitoring.

Authors

Michele Scagliarini

Department of Statistical Science, University of Bologna, Italy

Nunzia Boccaforno

Azienda Unità Sanitaria Locale della Romagna, Italy

Marco Vandi

Azienda Unità Sanitaria Locale della Romagna, Italy

Address for correspondence:

Dipartimento di Scienze Statistiche, Università di Bologna

Via Belle Arti 41, 40126, Bologna, Italy

Telephone number: +39 051 2098192

e-mail: michele.scagliarini@unibo.it

Title

Comparison of Control Charts for Poisson Count Data in Healthcare Monitoring.

Abstract

Statistical surveillance is a noteworthy endeavor in many healthcare areas such as epidemiology, hospital quality, infection control and patient safety. For monitoring hospital adverse events the Shewhart u -control chart is the most used methodology. One possible issue of the u -chart is that in healthcare applications the lower control limit (LCL) is often conventionally set to zero as the adverse events are rare and the sample sizes are not sufficiently large to obtain LCL greater than zero. Consequently, the control chart loses any ability to signal improvements. Furthermore, as the area of opportunity (sample size) is not constant over time, the in-control and out-of-control run length performances of the monitoring scheme are unknown. In this article, on the basis of a real case and through an intensive simulation study, we first investigate the in-control statistical properties of the u -chart. Then we set up several alternative monitoring schemes with the same in-control performances and their out-of-control properties are studied and compared. The aim is to identify the most suitable control chart considering jointly: the ability to detect unexpected changes (usually worsening), the ability to test the impact of interventions (usually improvements), the ease of use and clarity of interpretation. The results indicate that the EWMA control chart derived under the framework of weighted likelihood ratio test has the best overall performance.

Keywords: Average Run Length; Control Charts; Healthcare; Simulation Studies; Rare Events.

1 Introduction

Statistical methods for monitoring the occurrence rates of rare events are needed and used in many real world applications. To detect changes in the rate of an event, both the count of events recorded at regular time intervals and the corresponding sample size should be available and situations where the area of opportunity (sample size) is not constant over time are very common. Examples include the monitoring of non-conformities in batches with varying batch size, the monitoring of monthly rates of hospital acquired infections when the size of the at-risk population changes from month to month or monitoring of the incidence of a disease in a changing population (Woodall¹, Woodall and Montgomery² and Woodall and Driscoll³).

Control charts are effective methods in statistical process control for the continuous surveillance of rare events data in cases with varying sample sizes. The usual approach consists in modelling the count of events through independent Poisson random variables; therefore, detecting a change in the rate of occurrence can simply be achieved by detecting a change in the Poisson mean (Ryan and Woodall⁴, Shen *et al*⁵, Montgomery⁶).

In the healthcare framework, as for example for monitoring hospital adverse events, the Shewhart *u*-control chart (Montgomery⁶) is probably the most used methodology (Mohammed *et al*⁷). It is usually set up after performing a Phase I analysis in which the process parameters are estimated and the control limits are calculated from historical in-control data. In real applications the control limits are typically established using the 3-sigma rule (Mohammed *et al*⁷, Woodall *et al*⁸).

The *u*-control chart has several shortcomings. For example, it is not sensitive enough to detect small parameter shifts in real-time monitoring.

To improve the detection capability relative to that of the Shewhart control charts, several alternative monitoring schemes have been developed. Among them, the cumulative sum (CUSUM) and the exponentially weighted moving average (EWMA) charts are popular (Montgomery⁶).

Another possible issue of the *u*-chart, especially when the area of opportunity (sample size) is not constant over time, is that the in-control and out-of-control performances of the monitoring scheme are in effect unknown.

Furthermore, since in healthcare the adverse events are rare and the sample sizes are not sufficiently large to obtain lower control limits (LCL) greater than zero, LCL is often conventionally set to zero. Consequently, the control chart may lose any ability to signal possible improvements. This could result in negative practical implications, as in the healthcare framework the interest is frequently to detect the impact of interventions, or new procedures,

designed for the improvement of performances. It could be argued that improvements (negative shifts) may be detected using the supplementary run rules (Zhang and Wu⁹). However, run rules to be used require an adequate statistical education, since may lead to a false alarm rates increase (Montgomery⁶).

In this article we focus on the use of control charts for monitoring hospital adverse event rates. On the basis of a real case and through an intensive simulation study we first investigate the in-control properties of the Shewhart u -control chart. In this way we are able to assess whether the false alarm rate is acceptable for the current case study. It is worth noting that in real healthcare surveillance with non-constant area of opportunities, not only the u -chart, but also other monitoring algorithms, are often used without any discussion on their actual in-control statistical properties. Consequently, hospital performance assessments and/or decisions are based on the outcomes of a control chart on which there are no evaluations of its congruence with the task to be performed.

Then we set up several alternative EWMA monitoring schemes with the same in-control (IC) performances as the u -control chart. Specifically, we considered the EWMA control charts proposed by Dong *et al*¹⁰ (EWMAD), the version with a lower reflecting barrier by Ryan and Woodall⁴ (EWMARW), a proposal of ours based on the one of Dong *et al*¹⁰, but with a different variance (EWMAB), and finally the EWMA control chart derived under the framework of the weighted likelihood ratio test proposed by Zhou *et al*¹¹ (WEWMA). Here we limit ourselves to EWMA-type control charts given the easy implementation and interpretation.

The aim is to identify the most suitable control chart considering jointly: the ability to detect unexpected changes (usually worsening), to test the impact of interventions (usually improvements) and the ease of use and clarity of interpretation. The results indicate that the EWMA control chart derived under the framework of the weighted likelihood ratio test has the best overall performance.

The paper is organised as follows. In Section 2, we illustrate the case study, introduce some related open issues and compare the control charts on the basis of a real dataset. In Section 3, we review the theoretical background of the considered monitoring algorithms, use Monte Carlo simulations to study the in-control statistical properties of the u and EWMA charts and compare their out-of-control (OC) performances. Finally, Section 4 contains our concluding remarks.

All the simulations and the Figures of this paper are performed using *R*, (*R* core team)¹².

2 The case study and some open issues.

Patient falls are one of the most frequent adverse events in health care institutions (Chang *et al*¹³). A patient fall often causes serious consequences such as an increase in the period of hospitalization and a reduction in quality of life of the person that suffered the fall. Furthermore such an event increases hospital costs and can result in legal disputes. In order to ensure patient safety, evidence-based systems are implemented and the monitoring of adverse events constitutes one of an array of methods used by hospital management teams in pursuing safety in healthcare institutions (Baker *et al*¹⁴).

The Local Healthcare Authority of Romagna (Azienda Unità Sanitaria Locale, or AUSL, della Romagna) serves a population of around 1,124,896 inhabitants (the provinces of Forlì-Cesena, Ravenna and Rimini in Italy), employs 14,789 staff and houses 3,355 inpatient beds.

The Local Healthcare Authority of Romagna, in collaboration with the Department of Statistical Sciences of the University of Bologna, has started a quality improvement project aimed at improving process understanding and increasing patient safety and, considering the relevance of the “fall event” in the healthcare context, gave priority to the monitoring of monthly fall rates in its hospitals. The project involved 29 Hospital units, among these, without loss of any generality, we considered the hospital “Unit 1” of the “Infermi Hospital” in Rimini.

An inpatient fall, as the majority of adverse events in the healthcare framework, has the following peculiarities: it is a rare event and the area of opportunity, i.e. the size of the at-risk population, is not constant over time (Mohammed *et al*⁷).

We considered the inpatient fall-related adverse events data collected by the Hospital Patient-Safety reporting System for the period ranging from January 2014 to September 2019. The data are shown in Table 1 where for each month the number of falls (x_i) are reported together with the number of patient days (n_i^*).

[TABLE 1 APPROXIMATELY HERE]

To monitor the adverse event in question a u -chart for the number of falls per 1000 patient-days was implemented. Please note that the methodological and mathematical details of the the u -chart, as well as for the EWMA monitoring schemes presented in this paper, are reported in Section 3 below.

The u -control chart plots the statistic $u_i = (x_i/n_i)$ where $n_i = n_i^*/1000$ and to estimate the unknown falls rate θ_0 a “Phase I” was performed on the January 2014 – January 2016 period

($m=25$ months). Figure 1 (left side calibration data) shows the u -chart obtained using the R package “qcc” (Scrucca¹⁵) for the $m=25$ preliminary samples of Phase I.

[FIGURE 1 APPROXIMATELY HERE]

Before analyzing the results it is important to check for possible departure from the assumption of Poisson distributed data. This is a key issue since concerns the above reported u -chart, the EWMA-based monitoring schemes that will be examined in this article and all the simulation experiments that we are going to use in order to study and compare the statistical properties of the monitoring algorithms. The Poisson distribution depends on a single parameter, which is the mean as well as the variance (equidispersion). Problems can arise when the observations show more variability than would be expected by chance alone, since control charts, which are constructed on the basis of the standard Poisson distribution, on overdispersed data could produce high false alarm rate and misleading results. We used the goodness-of-fit test for discrete data based on the likelihood ratio statistic discussed in Friendly¹⁶ and implemented in the R package “vcd” (Meyer *et al*¹⁷). The hypothesis of Poisson distribution was tested on the 25 preliminary samples of Phase I and we obtained a likelihood ratio test statistic $G^2=1.369$, which with 3 degrees of freedom has a p -value=0.713. We completed the picture on the distribution issue also by testing for the presence of overdispersed data. In this case we used the test introduced by Wetherill and Brown¹⁸ and suitably implemented in the R package “qcc” (Scrucca¹⁵). The test statistic is distributed as a Chi-square distribution with (number of observations-1) degrees of freedom. The obtained result was $D=19.003$ with a corresponding p -value=0.75183. Summarizing, the hypothesis of Poisson distributed data was not rejected.

As the $m=25$ samples of Phase I did not show any out-of-control signals or particular systematic patterns we deem $\hat{\theta}_0 = 1.745708$ to be a reliable estimate of the monthly fall rate for 1000 patient days and the obtained control chart can be used for ongoing monitoring (Phase II) with data taken successively over time (Figure 1 right side). By examining the control chart of Figure 1 it can be noted that the fall rate remained relatively stable in the monitored period (February 2016-September 2019).

There are several issues that should be taken into account in connection with the above u -control chart. It can be noted that the lower control limit is zero. Therefore, potential decrements in the fall rate (*i.e.* improvements in hospital performance) cannot be reported by the control chart as alarm signals. However, for the purpose of completeness, we remind the reader that negative shifts could be detected using the supplementary run rules (Montgomery⁶), but with the typical

limitations of the sensitizing rules of the Shewhart control charts and with the concern that staff poorly trained in statistics could interpret the control charts incorrectly.

The other relevant issue is that the IC and OC performances of the chart are in effect unknown. This lack of knowledge on how often a false alarm should be expected and on the chart's shift detection ability could lead to difficulties or errors in the interpretation of the monitoring algorithm's outcomes.

A detailed investigation on the statistical properties of the u -chart, as well as for the EWMA-charts examined in this article, will be developed in the next Section. Here, to continue the analysis of the case study and to discuss whether the IC statistical properties of the Shewhart u -chart are adequate for the current monitoring task, we use some results obtained from the aforementioned investigation.

What resulted is that the IC average run length of the u -chart is $ARL_0 \cong 151$. Bearing in mind that a false alarm could divert some of the already scarce resources, that in overworked hospital units when alarms are excessive important signals are likely to be ignored together with irrelevant ones (Burkom¹⁹) and considering that we are dealing with monthly data, this value of IC ARL can be considered to be acceptable for the case at hand.

Therefore, for comparison purposes we set up the EWMAD, EWMAB, EWMARW, WEWMA (for positive shifts) and WEWMA (for negative shift) control charts with the same in-control performance as the u -chart. The results for the period monitored – February 2016 to September 2019 – are shown in Figures 2-6.

[FIGURE 2 APPROXIMATELY HERE]

[FIGURE 3 APPROXIMATELY HERE]

[FIGURE 4 APPROXIMATELY HERE]

[FIGURE 5 APPROXIMATELY HERE]

[FIGURE 6 APPROXIMATELY HERE]

To comment these results it is worth remembering that the monitoring actually began in the autumn of 2018. Since then, each hospital unit has a Shewhart u -control chart for monitoring the monthly fall rates. The fact of having monthly feedback on patient fall rates most probably placed a greater attention on the phenomenon leading to an improvement, albeit slight, in the performances. This could explain the results obtained: the most sensitive algorithm, the WEWMA (for negative shifts) control chart signalled a reduction in the fall rate in July 2019 whereas the other monitoring schemes did not detect any change.

3 Theoretical Background and Performance Comparisons

In healthcare surveillance a common situation is to monitor an incidence rate in cases where the area of opportunity of the event of interest is not constant over time: as for example the monitoring of an adverse event when the size of at-risk population changes randomly from month to month.

The issue of statistical monitoring of an event's occurrence rate with varying population sizes over time can be formalized as follows.

Let $X_1, X_2, \dots, X_i \dots$ be a sequence of event counts observed during fixed time periods. We assume that the X_i 's are independent Poisson observations with mean $n_i\theta_0$, where θ_0 is the incidence rate of the event in question and $n_1, n_2, \dots, n_i \dots$ are the sizes of the population at time i , respectively.

It is assumed that θ_0 changes to another unknown value θ_1 at some unknown time t_c and the objective is to detect the change as early as possible while controlling the false alarms rate.

3.1 The u -control chart

The Shewhart u -control chart is the simplest and probably the most used, monitoring algorithm for handling such changes in the area of opportunity (*i.e.* the changes in sample sizes). The u -chart is based on the average number of non-conformities (or adverse events) per inspection unit, *i.e.* $u_i = (X_i/n_i)$ with central line and control limits (with the usual 3-sigma rule) given by

$$CL = \theta_0 \quad (1)$$

$$LCL_i = \theta_0 - 3\sqrt{\theta_0/n_i} \quad (2)$$

$$UCL_i = \theta_0 + 3\sqrt{\theta_0/n_i} \quad (3)$$

respectively (Montgomery⁶). When the calculated lower control limit falls below zero it is customarily reset to zero because count data cannot fall below zero (Mohammed *et al*⁷). The u -chart signals an out-of-control situation when one of the plotted points u_i exceeds the control limits.

In practice the parameter θ_0 is often unknown and therefore should be estimated by performing a "Phase I" on m in-control-samples. In this case the estimator of θ_0 is

$$\hat{\theta}_0 = \left(\sum_{i=1}^m x_i / \sum_{i=1}^m n_i \right) \quad (4)$$

and the estimated value $\hat{\theta}_0$ replaces θ_0 in the above formulae.

One drawback of the Shewhart u -control chart is that it is not sensitive enough to detect small parameter shifts in real-time monitoring since the decision is based on the current value of the plotted statistic. Therefore, more sensitive alternatives such as the cumulative sum (CUSUM) and the exponentially weighted moving average (EWMA) control charts, which are based on past information along with current data, have been proposed in literature (Montgomery⁶). In what follows we examine several EWMA control schemes.

3.2 The EWMAD control chart

The first EWMA method under examination was proposed by Dong *et al*¹⁰. The EWMA statistic, in the following EWMAD, is

$$Z_i = \lambda_D \frac{X_i}{n_i} + (1 - \lambda_D) Z_{i-1} \quad (5)$$

where $\lambda_D \in (0,1]$ is a smoothing parameter, which determines the weights assigned to the past observations, and $Z_0 = \theta_0$. The exact variance of the EWMAD is

$$\sigma_{D_i}^2 = \lambda_D^2 \sum_{j=1}^i (1 - \lambda_D)^{2i-2j} \frac{\theta_0}{n_j} \quad (6)$$

and the bidirectional version of the EWMAD is

$$UCL_i = \theta_0 + L_D \sqrt{\sigma_{D_i}^2} \quad (7)$$

$$CL = \theta_0 \quad (8)$$

$$LCL_i = \theta_0 - L_D \sqrt{\sigma_{D_i}^2} \quad (9)$$

The factor L_D is the width of the control limits. It is possible to choose the design parameters λ_D and L_D that provide the desired average run length (ARL) performance of the chart. A reasonable, often-used rule of thumb is to choose $\lambda_D \in [0.05, 0.2]$ and to look for the control limits coefficient L_D to achieve a specific value of the IC ARL. In practice $\lambda_D = 0.05$, $\lambda_D = 0.1$ and $\lambda_D = 0.2$ are the most used values.

The EWMA methods were developed for Phase II monitoring. When the parameter θ_0 is unknown it can be estimated through a Phase I usually performed using a Shewhart u -chart. Dong *et al*¹⁰ also explored two other versions of their EWMA method based on the exact maximum value of the EWMAD variance

$$\sigma_{D_i}^{*2} = \frac{\theta_0}{n_0} \frac{\lambda_D}{2 - \lambda_D} \left[1 - (1 - \lambda_D)^{2i} \right] \quad (10)$$

and on the asymptotic maximum value of the EWMAD variance

$$\sigma_D^{*2} = \frac{\theta_0}{n_0} \frac{\lambda_D}{2 - \lambda_D} \quad (11)$$

respectively.

In the above formulae n_0 is the minimum sample size among all the values of n_i . However, the EWMA charts were mainly developed as Phase II methods, therefore, as Ryan and Woodall⁴ noted, there is no justification to consider (10) and (11), since it is not possible to know beforehand the minimum sample size as the samples are taken or observed in real time.

3.3 The EWMAB control chart

A possible solution that overcomes the problem related to the unknown n_0 is to use a modified version of the variance $\sigma_{D_i}^{*2}$ (10) by substituting n_0 with the current sample size n_i :

$$\sigma_{B_i}^{*2} = \frac{\theta_0}{n_i} \frac{\lambda_B}{2 - \lambda_B} \left[1 - (1 - \lambda_B)^{2i} \right] \quad (12)$$

In such a way we include, even if slightly modified, one of Dong *et al*¹⁰ proposals. Note that since the variance (12) uses the current sample size n_i , it leads to less smoothed control limits which might contribute to increase chart's detection capability.

The EWMA statistic, in the following EWMAB, is

$$Z_i^* = \lambda_B \frac{X_i}{n_i} + (1 - \lambda_B) Z_{i-1}^* \quad (13)$$

and the control limits of the EWMAB-chart are

$$UCL_i = \theta_0 + L_B \sqrt{\sigma_{B_i}^{*2}} \quad (14)$$

$$LCL_i = \theta_0 - L_B \sqrt{\sigma_{B_i}^{*2}} \quad (15)$$

where $\lambda_B \in (0,1]$, and $Z_0 = \theta_0$. Also in this case, the design parameters λ_B and L_B can be chosen in such a way as to obtain the desired ARL performance of the chart.

3.4 The EWMARW control chart

Ryan and Woodall⁴, to avoid a possible problem of inertia in detecting increases in the incidence rate, modified the EWMA control chart by introducing a lower reflecting barrier at $Z_i = \theta_0$. Their proposed EWMA statistic, in the following EWMARW, is

$$Z'_i = \max \left\{ \theta_0, \lambda_{RW} \frac{X_i}{n_i} + (1 - \lambda_{RW}) Z'_{i-1} \right\} \quad (16)$$

where $\lambda_{RW} \in (0,1]$ and $Z'_0 = \theta_0$. The upper control limit is given by

$$UCL_i = \theta_0 + L_{RW} \sqrt{\lambda_{RW}^2 \sum_{j=1}^i (1 - \lambda_{RW})^{2i-2j} \frac{\theta_0}{n_j}} \quad (17)$$

Also for the EWMARW, λ_{RW} and L_{RW} can be chosen as to obtain the desired ARL performance of the chart.

3.5 The WEWMA control chart

Zhou *et al*¹¹ proposed an EWMA control chart (WEWMA) derived under the framework of a weighted likelihood ratio test WLRT for monitoring Poisson count data with varying sample size. For the authors the monitoring task is to test $H_0 : \theta = \theta_0$ versus $H_1 : \theta = \theta_1$. By ignoring two constant terms with respect to θ , the log-likelihood of the observation X_j can be expressed as

$$l_j(\theta) = X_j \log \theta - n_j \theta \quad (18)$$

At any time point t , consider the following exponentially weighted log-likelihood over samples 1 to t

$$Y_t(\theta; \lambda_z) = \sum_{j=0}^t \omega_{j, \lambda_z} l_j(\theta) \quad (19)$$

where $\lambda_z \in (0,1]$ is the smoothing parameter, and $\omega_{j, \lambda_z} = \lambda_z (1 - \lambda_z)^{t-j}$ is a sequence of constants to ensure that all the weights add up to 1 as $t \rightarrow \infty$. For $j=0$, (X_0, n_0) can be viewed as a pseudo

“sample” and is chosen as $(n_1\theta_0, n_1)$. Given the value of λ_z , the maximum weighted likelihood estimate (MWLE) of θ at time point t is defined as the solution to the following maximization problem

$$\hat{\theta}_t = \arg \max_{\theta} Y_t(\theta; \lambda_z) \quad (20)$$

Since $\hat{\theta}_t$ can be written as (Zhou *et al*¹¹)

$$\hat{\theta}_t = \frac{\sum_{j=0}^t \omega_{j,\lambda} X_j}{\sum_{j=0}^t \omega_{j,\lambda} n_j} = \frac{Y_{c,t}}{Y_{p,t}} \quad (21)$$

it follows that the $-2 \times \log$ of weighted LRT (WLRT) statistic is

$$R_{t,\lambda_z} = 2 \left[Y_{c,t} \log \frac{Y_{c,t}}{\theta_0 Y_{p,t}} - Y_{c,t} + \theta_0 Y_{p,t} \right] \quad (22)$$

where $Y_{c,t}$ and $Y_{p,t}$ are the exponentially weighted average of counts and populations, respectively. The WLRT statistic R_{t,λ_z} can thus be used for monitoring and the corresponding control chart triggers a signal if R_{t,λ_z} exceeds a specified control limit. Note that $Y_{c,t}$ and $Y_{p,t}$ can be written according to the recursive formulations

$$Y_{c,t} = \lambda_z X_j + (1 - \lambda_z) Y_{c,t-1} \quad (23)$$

$$Y_{p,t} = \lambda_z n_j + (1 - \lambda_z) Y_{p,t-1} \quad (24)$$

where the initial values are $Y_{c,0} = \theta_0 n_1$ and $Y_{p,0} = n_1$ respectively based on the pseudosample (X_0, n_0) defined earlier. The chart can be implemented for detecting positive and negative shifts.

For positive shifts, $H_0 : \theta = \theta_0$ versus $H_1 : \theta > \theta_0$, the monitoring test statistic is

$$R_{t,\lambda_z}^* = R_{t,\lambda_z} I(\hat{\theta}_t > \theta_0) \quad (25)$$

and the WEWMA control chart is

$$T_{WEWMA} = \min \left\{ t; R_{t,\lambda_z}^* > L_{z,p} \frac{\lambda_z}{2 - \lambda_z}, t \geq 1 \right\} \quad (26)$$

where $L_{z,p} > 0$ is chosen to achieve a specific value of IC ARL.

For negative shifts, $H_0 : \theta = \theta_0$ versus $H_1 : \theta < \theta_0$ the monitoring test statistic is $R_{t,\lambda_z}^* = R_{t,\lambda_z} I(\hat{\theta}_t < \theta_0)$ and the WEWMA control chart is

$$T_{WEWMA} = \min \left\{ t; R_{t,\lambda_z}^* > L_{z,n} \frac{\lambda_z}{2 - \lambda_z}, t \geq 1 \right\} \quad (27)$$

where $L_{z,n} > 0$ and is chosen to achieve a specific value of IC ARL.

Also for the WEWMA a reasonable rule-of-thumb used in practice for designing the control chart is to choose $\lambda_z \in [0.05, 0.2]$ and to look for the control limits coefficient $L_{p,n}$ (or $L_{z,n}$) to achieve a specific value of the IC ARL.

3.6. IC Performance of the u -Control Chart

There are several measures for assessing the IC properties of monitoring algorithms. The most commonly used measure is the average run length (ARL) when there is no change in the system under surveillance.

The run length of a control chart is a discrete random variable that is defined as the number of plotted statistics before an out-of-control point is observed on the chart. The ARL is the expected value of this random variable.

Here we study the IC run length distribution of the u -chart by means of a simulation experiment based on $k=50000$ replications.

In detail we simulated observations from a Poisson distribution with parameter $\hat{\theta}_0 n_i$, *i.e.* $x_i \sim Po(\hat{\theta}_0 n_i)$. The varying sample sizes n_i used for the simulations were generated from a uniform distribution $U(a, b)$ with $a = \min(n_{ii})/1.5$, $b = 1.5 \cdot \max(n_{ii})$, where $\min(n_{ii})$ and $\max(n_{ii})$ are the minimum and the maximum of the sample sizes $n_i = n_i^*/1000$ of the in-control data of Phase I, respectively. Note that, in this manner two goals were achieved: i) no particular changing patterns are assumed for the sample sizes, thereby this “neutral scenario” ensures that the varying n_i had no systematic effect on the IC performance of the chart; ii) through the extension of the distribution’s support $[a, b]$, by 50% with respect to both the minimum and maximum of the sample sizes we are able to simulate the sample sizes over a wide and realistic range of possible values.

For each run of the k replications the observations are generated until $u_i \geq UCL_i$. The first i for which $u_i \geq UCL_i$ is the in-control RL. The average of the k RLs is our estimate of the IC ARL (ARL_0). It is important to remember that when a control chart is developed with estimated parameters, to summarize the run length distribution using only the ARL can be misleading (Ryan and Woodall⁴, Jones *et al*²⁰, Mei²¹). Therefore we complete the picture of the IC control chart performance by also computing the 10th percentile $Q(0.10)$, the median, the 90th percentile $Q(0.90)$ of the marginal distribution of the run length, the standard deviation of the run length (SDRL) and the false alarm rate (FAR) for the first 30 observations. The results are reported in Table 2.

[TABLE 2 APPROXIMATELY HERE]

The IC run length distribution of a control chart is considered to be satisfactory if it is close to the geometric distribution or more generally if it varies to a lesser extent than the geometric distribution (Hawkins and Olwell²²). As a reference, when the run length distribution is geometric with an expected value equal to 151.168, the SDRL should be approximately equal to ARL_0 , and $Q(0.10)$, Median, $Q(0.90)$, and FAR should be approximately 16, 104, 347, and 0.181, respectively. From the results of Table 2 it can be noted that SDRL, $Q(0.10)$, $Q(0.90)$, Median, and FAR are all approximately equal to the respective theoretical values. Therefore, the geometric distribution is a fairly reasonable approximation to the IC run length distributions of the u -chart. This means that the IC behavior of the u -chart complies with the theoretical expectations and the ARL_0 is a suitable summary of its IC run behavior.

3.7. Set-up of the EWMA control charts

To perform the comparisons all the charts examined must have the same IC performance. Here we introduce the simulation-based procedure designed to set up the EWMAD, EWMAB, EWMARW and the WEWMA control charts with the same IC performance as the u -chart.

For convenience we used the same value for the smoothing parameter $\lambda_D = \lambda_B = \lambda_{RW} = \lambda_z = 0.1$ and by means of an iterative search algorithm, based on $k=50000$ simulations we looked for the parameters L_D , L_B , L_{RW} , $L_{z,p}$ and $L_{z,n}$ that allow us to achieve the same IC ARL (151.168) as in the u -chart.

The algorithm works as follows:

- 1) with an initial value for L_D (L_B , L_{RW} , $L_{z,p}$ or $L_{z,n}$) denoted by L_{start} the empirical ARL_0 is estimated as the average of $k=50000$ RLs values obtained by simulating observations under H_0
- 2) If $ARL_0 \in [151.168 \pm 5\%]$ then L_D (L_B , L_{RW} , $L_{z,p}$ or $L_{z,n}$) is set equal to L_{start} and the search algorithm stops
- 3) Otherwise, if $ARL_0 > 151.168$, then $L_{start} = L_{start} - 0.05$; if $ARL_0 < 151.168$, then $L_{start} = L_{start} + 0.05$ and the algorithm starts other k simulations.

The results are summarized in Table 3.

[TABLE 3 APPROXIMATELY HERE]

Examining the results reported in Table 3 it can be seen that the geometric distribution is a reasonable approximation to the IC run length distribution for all the EWMA-type control charts examined. This confirms that the examined EWMA charts work well under the IC condition and for these charts the ARL is a suitable summary of their IC run behavior.

3.8. OC performance comparison

All the control charts examined are designed to achieve the same IC ARL; therefore we are able to study and compare their OC performance. For this purpose, we designed a simulated experiment where the observations are generated from a Poisson distribution with parameter $\theta_1 n_i$ for different values of θ_1 . As values for θ_1 we considered cases where the in-control parameter $\hat{\theta}_0$ had been increased by 2.5%, 5%, 10% and up to 100% with steps of 10% while the varying sample sizes n_i were generated from a uniform distribution $U(a, b)$ as explained in Section 3.6. Once again it is important to point out that in this way we assumed a neutral scenario for the sample sizes and attention was focused on the effects of a change in the fall-rate parameter. For each run of the $k=50000$ simulations we generated observations until u_i (Z_i , Z_i^* , Z_i' or R_{t, λ_c}^*) was lower than the corresponding upper control limit. The first i (or t) for which the test statistic exceeded the UCL was the out-of-control RL. The average of the 50000 RLs is our estimate of the ARL_1 . Please note that all the comparisons are made in terms of steady-state ARL (Ryan and Woodall⁴, Zhou *et al*¹¹). The results are summarized in Table 4.

[TABLE 4 APPROXIMATELY HERE]

To assess the overall performance of these charts we also computed their relative mean index (RMI) values. The RMI index assesses the overall performance of a monitoring algorithm by providing an average measure of relative efficiency. RMI is defined as (Han and Tsung²³)

$$RMI = \frac{1}{N} \sum_{i=1}^N \frac{ARL_{\delta_i} - MARL_{\delta_i}}{MARL_{\delta_i}} \quad (28)$$

where N is the total number of shifts considered, ARL_{δ_i} is the OC ARL of the given control chart when detecting a parameter shift of magnitude δ_i , and $MARL_{\delta_i}$ is the smallest among all OC ARL values of the charts considered when detecting the shift δ_i . The control chart with a smaller RMI has the best overall performance. For positive shifts the RMI values are reported in the last row of Table 4.

The WEWMA control chart is designed to detect both positive and negative shifts, however in the problem under study the EWMAD and EWMAB are able to detect negative shifts, since it can be shown that the sample size required to obtain negative lower control limits should be smaller than 1.

Let us examine the EWMAD control chart. Regarding the sample size n_i as an unknown quantity, n_u , and considering the asymptotic maximum value of the EWMAD variance (11) we

can solve the inequality $LCL_{asymptotic} = \theta_0 - L_D \sqrt{\frac{\theta_0}{n_u} \frac{\lambda_D}{2 - \lambda_D}} \leq 0$ with respect to the unknown n_u .

The result is $n_u \leq \frac{L_D^2}{\theta_0} \frac{\lambda_D}{2 - \lambda_D}$. In our case, with $\theta_0 = 1.745708$, $L_D = 2.35$ and $\lambda_D = 0.1$ we

obtain $n_u \leq 0.1665$. For the EWMAB chart ($L_B = 2.6$), by a similar approach, the result is $n_u \leq 0.2038$.

Therefore, we also studied the statistical properties of these charts for the case of a decrease in the incidence rate. The simulation experiment was designed as for positive shifts. The observations are generated from a Poisson distribution with parameter $\theta_1 n_i$ for different values of θ_1 . As values for θ_1 we considered cases where the in-control parameter $\hat{\theta}_0$ had been decreased by 2.5%, 5%, 10% and up to 100% with steps of 10%. Also in this case, the varying sample sizes n_i were generated from a uniform distribution $U(a, b)$ as explained in Section 3.6. The results are summarized in Table 5.

[TABLE 5 APPROXIMATELY HERE]

The results reveal that for positive shifts, the EWMAB-chart has a performance that is very similar to the EWMAD-chart. The RMI values are 0.1166 and 0.1491 for the EWMAD and EWMAB charts, respectively (Table 4). For negative shifts, the EWMAB-chart shows a slightly better detection ability than the EWMAD-chart. For example, a 10% decrease in the rate is detected by the EWMAB-chart after 113 months on average, while the EWMAD-chart signals the same shift after 128 months. For negative shifts the RMIs are 0.4791 and 0.4305 for the EWMAD and EWMAB charts, respectively (Table 5). These results suggest that the use of variance (12) might have contributed to the improvement of the control chart performance.

For detecting positive shifts, due to the introduction of the lower reflecting barrier, the EWMARW-chart performs better than the EWMAB and EWMAD charts and for $\theta_1 \geq \theta_0 + 0.6\theta_0$ performs slightly better than the WEWMA-chart (Table 4).

The WEWMA-chart outperforms all the other control charts for negative shifts and for positive shifts less than or equal to 50%.

For example, the WEWMA-chart detects a 5% increase in the rate after 85 months on average, the EWMARW after 93, the EWMAB like the EWMAD after 110, and the u -chart after 118.

Please note that the magnitudes of the shift (from |2.5|% to |100|%) in the falls rate $\hat{\theta}_0$ considered in this study represent, in our opinion, realistic scenarios for hospital fall count data. Therefore, the results obtained can be considered as a reasonable summarized picture of the performances of the examined monitoring algorithms.

4. Concluding remarks

Assessing changes in the outcome of a rare event that is subject to fluctuation in the at-risk population is challenging. In these cases it is important to use monitoring algorithms that are capable of handling such changes in the sample sizes.

For monitoring Poisson count data with varying sample sizes, the Shewhart u -chart, albeit with some limits, is the most accessible control chart, particularly in terms of setting up the chart.

In this article, based on a real dataset and using simulations to develop various realistic scenarios for healthcare count data, we have compared the u -chart with several EWMA monitoring schemes.

First, through a simulation study, the IC run length performance of the u -chart was studied to evaluate whether it was acceptable for the case under examination. With regard to this issue, it is worth noting that in real healthcare applications with varying sample size the evaluation of the in-control statistical properties of any control chart is often neglected. Consequently, hospital performance assessments and the resulting decisions are based on the outcomes of a monitoring algorithm without any discussion on its adequacy. We believe that to avoid errors and the wasting of resources it could be beneficial to estimate the baseline performance of the control chart being used and to discuss whether they are adequate for the current monitoring task.

Then, EWMA-charts, with the same IC performance as the u -chart, were implemented and compared on a real dataset. Furthermore, the OC statistical properties were studied by developing realistic scenarios for hospital fall count data using simulations.

Since in the healthcare field it is important not only to quickly identify an increase in the rate of adverse events but also to detect any improvement as a result of suitable interventions in comparing the control charts, both aspects have been taken into account.

The results showed that the WEWMA-chart outperforms all the other control charts for negative shifts and for small positive shifts $\leq 50\%$. The EWMAB-chart has approximately the same performance as the EWMAD-chart. For detecting positive shifts, the EWMARW-chart performs better than the EWMAB and EWMAD charts and for relatively large increases ($\geq 60\%$) it has slightly better performance than the WEWMA-chart.

To summarise, due to its fast detection properties and the ability to detect shifts in both directions, the WEWMA control chart may represent a valuable tool for monitoring hospital adverse events.

A possible minor issue of the WEWMA-chart is that it lacks direct interpretability as the plotted statistic cannot be interpreted as an estimate of the current event rate. To overcome this problem, since simplicity, training issues and ease of interpretation of charts for healthcare teams are important aspects in order to avoid inappropriate decisions and to reduce fatigue, the Local Healthcare Authority of Romagna patient safety team opted for the joint use of the WEWMA and u -chart.

As stated in the Introduction, in this work we focused solely on the EWMA control charts. However, the CUSUM-type monitoring algorithms are also widely used for monitoring count data in many areas including the healthcare framework. We will consider the CUSUM-topic in a future piece of research.

It is also important to remember that control charts for monitoring count data are generally constructed under the assumption of Poisson distributed observations. Several studies (Jones and Govindaraju²⁴, Heimann²⁵, Laney²⁶, Spiegelhalter²⁷, Mohammed and Laney²⁸), however, argued that the underlying equidispersion assumption might not hold as practical cases with overdispersion or underdispersion should also be considered. Saghir and Lin²⁹ provided a comprehensive review of methodologies for monitoring dispersed count data and gave interesting ideas for possible future developments of the present research.

Finally, we are aware that the performance of the EWMA charts depends on the smoothing parameter λ , which, for the purposes of conciseness, has been set to a constant value in this article. Further pieces of research will be devoted to the role of the value of the λ on the examined EWMA charts.

Acknowledgements

We are grateful to the Editors and the Reviewers for very useful comments and suggestions.

References

1. Woodall WH. The Use of Control Charts in Health-Care and Public-Health Surveillance, with discussion. *J. Qual. Technol.* 2006; **38**:89-104.
2. Woodall, WH, Montgomery, DC. Some current directions in the theory and application of statistical process monitoring. *J. Qual. Technol.* 2014; 46:78-94.
3. Woodall WH, Driscoll AR. Some Recent Results on Monitoring the Rate of a Rare Event. In Knoth S., Schmid W. (Eds.) *Frontiers in Statistical Quality Control 11*. Springer International Publishing Switzerland 2015; 15-27.
4. Ryan AG, Woodall WH. Control charts for Poisson count data with varying sample sizes. *J. Qual. Technol.* 2010; **42**: 260-274.
5. Shen X, Zou C, Jiang W, Tsung F. Monitoring Poisson Count Data with Probability Control Limits when Sample Sizes are Time Varying. *Nav. Res. Logist.* 2013; **60**: 625-363.
6. Montgomery DC. *Introduction to Statistical Quality Control*, (7th Edition). John Wiley & Sons, Inc.: Hoboken, NJ, 2009.
7. Mohammed MA, Worthington P., Woodall, WH. *Tutorial notes on how to plot some basic control charts.* *Qual. Saf. Health Care* 2008; **17**: 137-145.

8. Woodall WH, Adams BM, Benneyan JC. The Use of Control Charts in Healthcare. In Faltin F, Kenett R., Ruggeri F. (Eds.) *Statistical Methods in Healthcare*. Wiley: New York, 2012; 253-267.
9. Zhang S, Wu Z. Designs of control charts with supplementary runs rules. *Computers & Industrial Engineering* 2005; **49**: 76-97.
10. Dong Y, Hedayat AS, Sinha BK. Surveillance Strategies for Detecting Change point in Incidence Rate Based on Exponentially Weighted Moving Average Methods. *J. Am Stat. Assoc.* 2008; **103**: 843-853.
11. Zhou Q, Zou C, Wang Z, Jiang, W. Likelihood-Based EWMA Charts for Monitoring Poisson Count Data With Time-Varying Sample Sizes. *J. Am Stat. Assoc.* 2012; **107**: 1049-1062.
12. R Core Team. *R: A language and environment for statistical computing*. R Foundation for Statistical Computing: Vienna, 2017.
13. Chang C-M, Kao C-H, Sha W-S, Wu W-H, Chen J-C. Multilevel control chart and fuzzy set theory to monitor inpatient falls. *J. Bus. Res.* 2016; **69**: 2284-2288.
14. Baker A, Morton A, Gatton, M, Tong E, Clements A. Sequential monitoring of hospital adverse events when control charts fail: The example of fall injuries in hospitals. *Qual. Saf. Health Care* 2009; **18**: 473-477.
15. Scrucca L. qcc: an R package for quality control charting and statistical process control. *R News*, 2004; **4**: 11-17.
16. Friendly M. *Visualizing Categorical Data*. SAS Institute: Cary, NC, 2000.
17. Meyer D., Zeileis A., Hornik K. *vcd: Visualizing Categorical Data*. R package version 1.4-6, 2020.
18. Wetherill, GB., Brown, DW. *Statistical Process Control*. Chapman and Hall: New York, 1991.
19. Burkom H. *Discussion* in Woodall WH. The Use of Control Charts in Health-Care and Public-Health Surveillance, with discussion. *J. Qual. Technol.* 2006, **38**:127-132.
20. Jones LA, Champ CW, Rigdon SE. The Performance of Exponentially Weighted Moving Average Charts With Estimated Parameters. *Technometrics* 2001; **43**: 156-167.
21. Mei Y. Is Average Run Length to False Alarm Always an Informative Criterion? (With Discussions). *Seq. Anal.* 2008; **27**: 354-419.
22. Hawkins DM, Olwell DH. *Cumulative Sum Charts and Charting for Quality Improvement*. Springer-Verlag: New York, 1998.

23. Han D., Tsung F. A Reference-Free Cuscore Chart for Dynamic Mean Change Detection and a Unified Framework for Charting Performance Comparison. *J. Am Stat. Assoc.*, 2006; **101**: 368-386.
24. Jones G, Govindaraju KA. Graphical method for checking attribute control chart assumptions. *Qual. Eng.* 2000; **13**:19-26.
25. Heimann PA. Attributes control charts with large sample sizes. *J Qual Technol.* 1996; **28**:451-4599.
26. Laney DB. Improved control charts for attribute data. *Qual Eng.* 2002;**14**: 531-537
27. Spiegelhalter D. Handling overdispersion of performance indicators. *Qual Saf Health Care* 2005;**14**: 347-351.
28. Mohammed, Laney DB. Overdispersion in health care performance data: Laney's approach. *Qual Saf Health Care* 2006; **15**: 383-384.
29. Saghir A., Lin Z. Control charts for dispersed count data: an overview. *Qual. Reliab. Eng. Int.* 2015; **31**: 725-739.

Table 1: x_i monthly falls and n_i^* patient days for the period January 2014-September 2019

| Month | n_i^* | x_i | Month | n_i^* | x_i | Month | n_i^* | x_i |
|--------|---------|-------|--------|---------|-------|--------|---------|-------|
| Jan-14 | 1271 | 1 | Dec-15 | 1058 | 2 | Nov-17 | 1487 | 3 |
| Feb-14 | 912 | 0 | Jan-16 | 1334 | 1 | Dec-17 | 1344 | 2 |
| Mar-14 | 1139 | 3 | Feb-16 | 1057 | 2 | Jan-18 | 1234 | 3 |
| Apr-14 | 959 | 2 | Mar-16 | 1251 | 1 | Feb-18 | 1435 | 3 |
| May-14 | 1112 | 1 | Apr-16 | 1118 | 3 | Mar-18 | 1277 | 1 |
| Jun-14 | 1029 | 2 | May-16 | 1089 | 3 | Apr-18 | 1277 | 1 |
| Jul-14 | 1019 | 2 | Jun-16 | 1123 | 1 | May-18 | 1450 | 1 |
| Aug-14 | 1046 | 0 | Jul-16 | 1097 | 1 | Jun-18 | 1347 | 3 |
| Sep-14 | 1002 | 1 | Aug-16 | 1009 | 2 | Jul-18 | 1238 | 1 |
| Oct-14 | 1201 | 0 | Sep-16 | 1193 | 3 | Aug-18 | 1424 | 4 |
| Nov-14 | 1062 | 3 | Oct-16 | 1026 | 2 | Sep-18 | 1395 | 2 |
| Dec-14 | 1090 | 5 | Nov-16 | 1087 | 3 | Oct-18 | 1382 | 4 |
| Jan-15 | 1363 | 2 | Dec-16 | 1144 | 2 | Nov-18 | 1423 | 3 |
| Feb-15 | 952 | 1 | Jan-17 | 1434 | 3 | Dec-18 | 1505 | 2 |
| Mar-15 | 1285 | 2 | Feb-17 | 1238 | 3 | Jan-19 | 1373 | 1 |
| Apr-15 | 992 | 3 | Mar-17 | 1373 | 1 | Feb-19 | 1390 | 0 |
| May-15 | 1192 | 3 | Apr-17 | 1277 | 1 | Mar-19 | 1106 | 2 |
| Jun-15 | 902 | 2 | May-17 | 1400 | 1 | Apr-19 | 1144 | 1 |
| Jul-15 | 1243 | 3 | Jun-17 | 1337 | 3 | May-19 | 1123 | 1 |
| Aug-15 | 1102 | 2 | Jul-17 | 1337 | 1 | Jun-19 | 1069 | 1 |
| Sep-15 | 1011 | 3 | Aug-17 | 1386 | 2 | Jul-19 | 1186 | 0 |
| Oct-15 | 1186 | 4 | Sep-17 | 1240 | 2 | Aug-19 | 1026 | 2 |
| Nov-15 | 1034 | 0 | Oct-17 | 1126 | 2 | Sep-19 | 1305 | 2 |

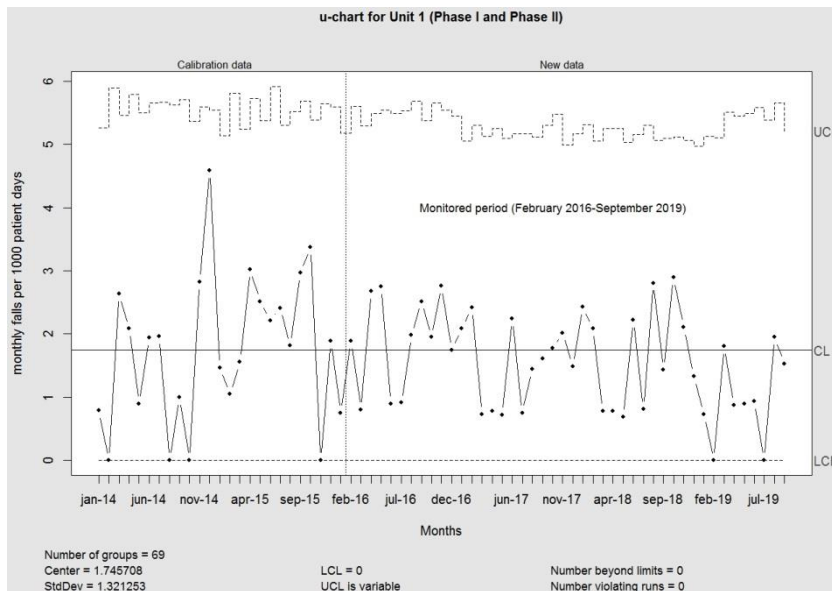


Figure 1: u -chart for Phase I (Calibration Data) and Phase II (New Data)

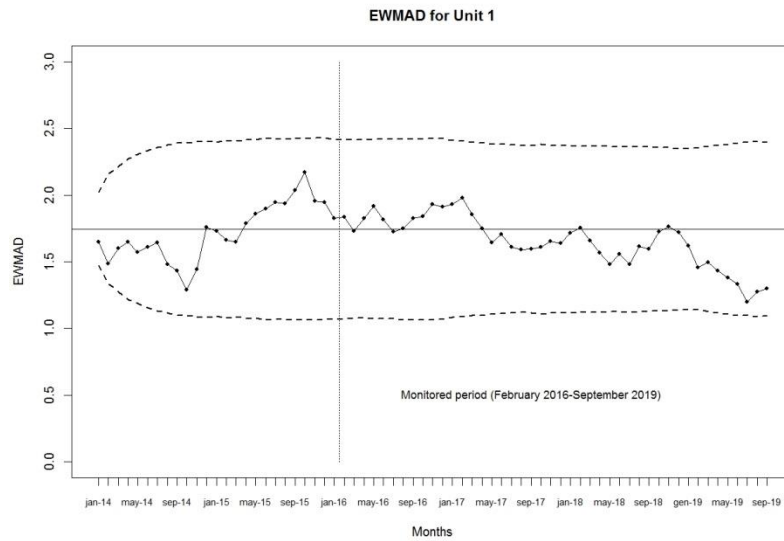


Figure 2: EWMAD control chart for monitoring the monthly fall per 1000 patient days

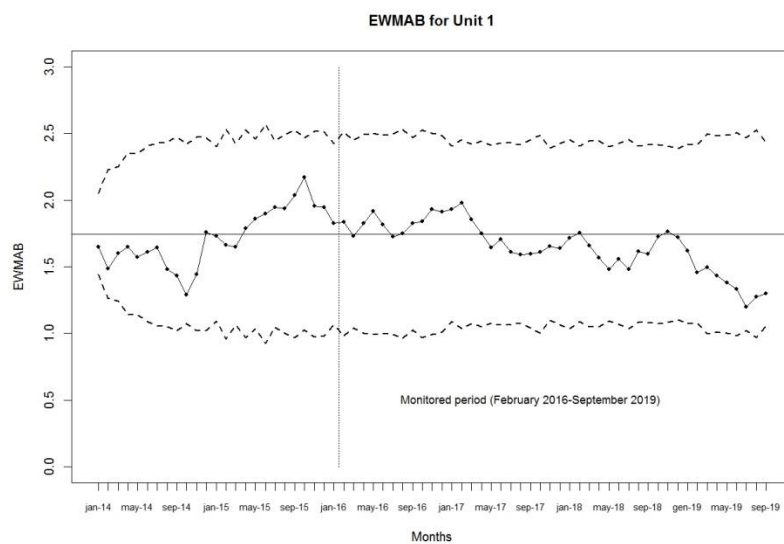


Figure 3: EWMAB control chart for monitoring the monthly fall per 1000 patient days

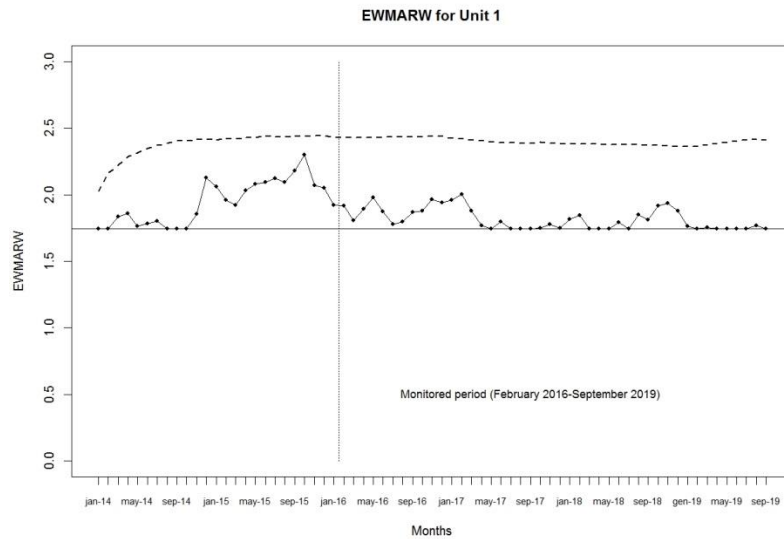


Figure 4: EWMARW control chart for monitoring the monthly fall per 1000 patient days

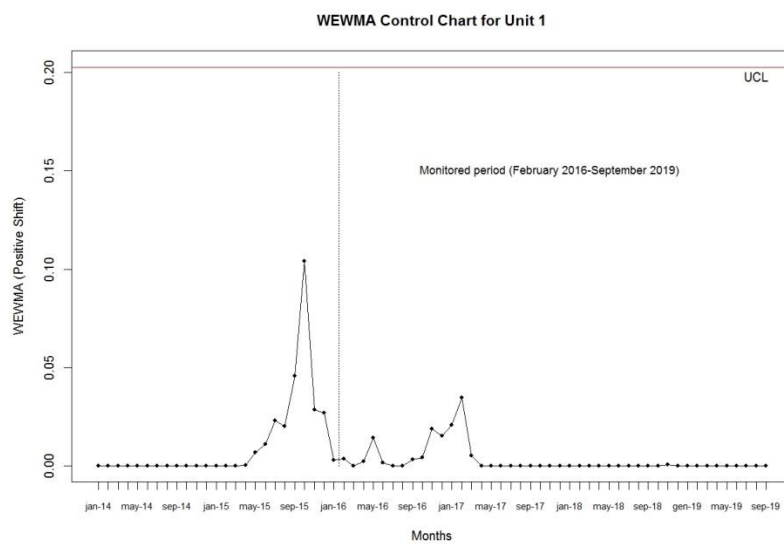


Figure 5: WEWMA control chart (positive) for monitoring the monthly fall per 1000 patient days

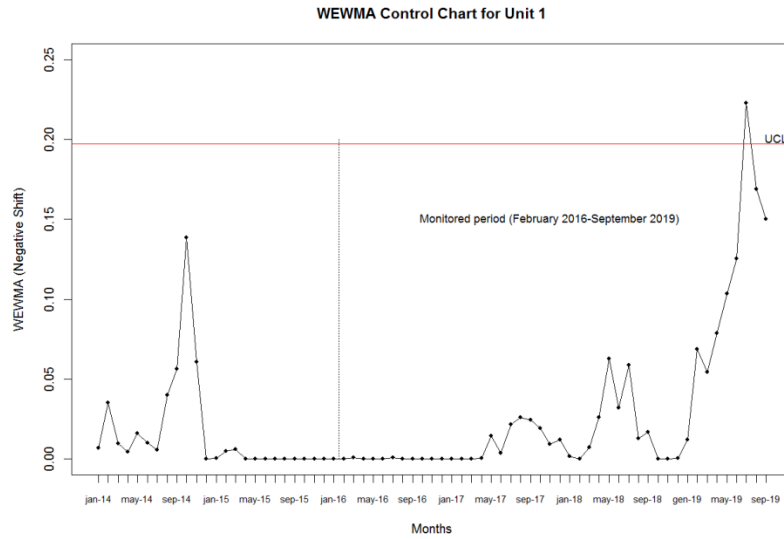


Figure 6: WEWMA control chart (negative) for monitoring the monthly fall per 1000 patient days

Table 2: IC RL results from the simulations

| ARL_0 | SDRL | $Q(0.10)$ | Median | $Q(0.90)$ | FAR |
|----------|----------|-----------|--------|-----------|--------|
| 151.1684 | 151.7784 | 16 | 104 | 348 | 0.1826 |

Table 3: IC Run Length Results ($ARL_0 \cong 151.168$)

| | L | SDRL | $Q(0.10)$ | Median | $Q(0.90)$ | FAR |
|--------|------------------|----------|-----------|--------|-----------|--------|
| EWMAD | $L_D = 2.35$ | 173.3981 | 11 | 98 | 361 | 0.2173 |
| EWMAB | $L_B = 2.6$ | 152.1211 | 13 | 101 | 345 | 0.1998 |
| EWMARW | $L_{RW} = 2.4$ | 158.1871 | 11 | 95 | 341 | 0.2180 |
| WEWMA | $L_{z,p} = 3.85$ | 144.7811 | 17 | 103 | 337 | 0.1787 |
| WEWMA | $L_{z,n} = 3.75$ | 143.0383 | 18 | 101 | 332 | 0.1767 |

Table 4: OC ARL results for positive shifts with standard deviations in parenthesis. RMIs in last row.

| θ | u -chart | EWMAD | EWMAB | EWMARW | WEWMA |
|---------------------------------------|------------------------|------------------------|------------------------|------------------------|------------------------|
| $\theta_1 = \theta_0 + 0.025\theta_0$ | 133.9905 (132.7186) | 132.1178 (147.8677) | 130.9323 (134.1310) | 115.3659 (125.9228) | 110.6871 (108.5948) |
| $\theta_1 = \theta_0 + 0.05\theta_0$ | 118.6586 (118.2208) | 110.0868 (121.8029) | 109.7551 (111.6834) | 92.7468 (100.6559) | 84.5281 (81.2703) |
| $\theta_1 = \theta_0 + 0.1\theta_0$ | 94.0243 (92.5185) | 73.1380 (78.6863) | 73.8657 (73.7917) | 61.4061 (64.9530) | 54.4491 (50.8256) |
| $\theta_1 = \theta_0 + 0.2\theta_0$ | 60.5622 (60.2563) | 35.2278 (35.3403) | 35.3529 (33.6384) | 31.5537 (31.9621) | 27.8345 (23.6924) |
| $\theta_1 = \theta_0 + 0.3\theta_0$ | 41.3927 (40.7772) | 20.3272 (19.2478) | 20.5224 (18.4503) | 19.0739 (18.2836) | 17.5386 (13.5072) |
| $\theta_1 = \theta_0 + 0.4\theta_0$ | 29.1579 (28.5864) | 13.2522 (12.0847) | 13.6281 (11.6449) | 12.7821 (11.6722) | 12.4624 (8.8792) |
| $\theta_1 = \theta_0 + 0.5\theta_0$ | 21.3988 (20.9510) | 9.4756 (8.338) | 9.8432 (8.0980) | 9.2430 (8.0653) | 9.5582 (6.3000) |
| $\theta_1 = \theta_0 + 0.6\theta_0$ | 16.2447 (15.7133) | 7.2777 (6.2156) | 7.6341 (6.0495) | 7.07910 (5.9804) | 7.7314 (4.7644) |
| $\theta_1 = \theta_0 + 0.7\theta_0$ | 12.4837 (11.9544) | 5.7699 (4.8123) | 6.1010 (4.7502) | 5.7215 (4.6926) | 6.4493 (3.7421) |
| $\theta_1 = \theta_0 + 0.8\theta_0$ | 9.9399 (9.4732) | 4.7654 (3.8853) | 5.0476 (3.8480) | 4.7233 (3.7778) | 5.6140 (3.1488) |
| $\theta_1 = \theta_0 + 0.9\theta_0$ | 8.1001 (7.5586) | 4.0696 (3.2181) | 4.3154 (3.1959) | 4.0651 (3.1682) | 4.9570 (2.6624) |
| $\theta_1 = \theta_0 + 1.0\theta_0$ | 6.6627 (6.1238) | 3.5041 (2.7230) | 3.7776 (2.7516) | 3.5139 (2.6596) | 4.4419 (2.3084) |
| RMI | 1.0006 | 0.1166 | 0.1491 | 0.0431 | 0.0774 |

Table 5: OC results for negative shifts with standard deviations in parenthesis

| θ | EWMAD | EWMAB | WEWMA |
|---------------------------------------|------------------------|------------------------|-----------------------|
| $\theta_1 = \theta_0 - 0.025\theta_0$ | 165.8823 (191.3911) | 154.8556 (156.7213) | 110.8259 (106.151) |
| $\theta_1 = \theta_0 - 0.05\theta_0$ | 165.3261 (191.3279) | 150.7474 (150.7520) | 85.3380 (80.6883) |
| $\theta_1 = \theta_0 - 0.1\theta_0$ | 127.5269 (143.2911) | 112.8251 (109.7253) | 54.2937 (48.2809) |
| $\theta_1 = \theta_0 - 0.2\theta_0$ | 55.3412 (52.9344) | 50.0287 (43.5181) | 26.4997 (20.6650) |
| $\theta_1 = \theta_0 - 0.3\theta_0$ | 27.6411 (22.2168) | 25.7524 (19.0283) | 15.8329 (10.3017) |
| $\theta_1 = \theta_0 - 0.4\theta_0$ | 16.2702 (10.9818) | 15.7219 (9.9151) | 10.8850 (5.8512) |
| $\theta_1 = \theta_0 - 0.5\theta_0$ | 10.8676 (6.2794) | 10.7659 (5.8794) | 8.2059 (3.7207) |
| $\theta_1 = \theta_0 + 0.6\theta_0$ | 7.8350 (3.9919) | 7.9465 (3.7671) | 6.5061 (2.5376) |
| $\theta_1 = \theta_0 + 0.7\theta_0$ | 5.9318 (2.6232) | 6.1581 (2.5096) | 5.3999 (1.7756) |
| $\theta_1 = \theta_0 + 0.8\theta_0$ | 4.6687 (1.7486) | 4.9846 (1.7596) | 4.6247 (1.3195) |
| $\theta_1 = \theta_0 + 0.9\theta_0$ | 3.7886 (1.1544) | 4.1282 (1.2210) | 4.0470 (1.0008) |
| $\theta_1 = \theta_0 + 1.0\theta_0$ | 3.1241 (0.9257) | 3.5102 (0.8310) | 3.6081 (0.7841) |
| RMI | 0.4791 | 0.4305 | 0.0186 |